Parallelization of Large-Scale Attack and Compliance Graph Generation Using Message-Passing Interface

Noah L. Schrick
Tandy School of Computer Science
The University of Tulsa
Tulsa, USA
noah-schrick@utulsa.edu

Peter J. Hawrylak
Tandy School of Computer Science
The University of Tulsa
Tulsa, USA
peter-hawrylak@utulsa.edu

***Abstract*—**

***Index Terms*—Attack Graph; Compliance Graph; MPI; High-Performance Computing; Cybersecurity; Compliance and Regulation; Speedup; Parallelism;**

I. Introduction

This work attempts to further those efforts and extend RAGE to function on distributed computing environments to take advantage of the increased computing power using message-passing. As mentioned by the author of [1], MPI is the most widely used message-passing API, and this work intended to utilize an API that was not only familiar and accessible, but versatile and powerful for parallelizing RAGE for distributed computing platforms. This work discusses a task parallelism approach for the generation process, and uses OpenMPI for the MPI implementation.

II. Related Works

For architectural and hardware techniques for general graph generation improvement, the authors of [2] discuss the high cache miss rate, and how general prefetching does not increase the prediction rate due to nonsequential graph structures and data-dependent access patterns. However, the authors continue to discuss that generation algorithms are known in advance, so explicit tuning of the hardware prefetcher to follow the traversal order pattern can lead to better performance. The authors were able to achieve over 2x performance improvement of a breadth-first search approach with this method. Another hardware approach is to make use of accelerators. The authors of [3] present an approach for minimizing the slowdown caused by the underlying graph atomic functions. By using the atomic function patterns, the authors utilized pipeline stages where vertex updates can be processed in parallel dynamically. Other works, such as those by the authors of [4] and [5], leverage field-programmable gate arrays (FPGAs) for graph generation in the HPC space through various means. This includes reducing memory strain, storing repeatedly accessed lists, storing results, or other storage through the on-chip block RAM, or even leveraging Hybrid Memory Cubes for optimizing parallel access.

From a data structure standpoint, the authors of [6] describe the infeasibility of adjacency matrices in large-scale graphs, and this work and other works such as those by the authors of [7] and [8] discuss the appeal of distributing a graph representation across systems. The author of [8] discusses the usage of distributed adjacency lists for assigning vertices to workers. The authors of [8] and [9] present other techniques for minimizing communication costs by achieving high compression ratios while maintaining a low compression cost. The Boost Graph Library and the Parallel Boost Graph Library both provide appealing features for working with graphs, with the latter library notably having interoperability with MPI, Graphviz, and METIS [10], [11].

There have also been numerous approaches at generation improvement specific to attack graphs. As a means of improving scalability of attack graphs, the authors of [12] present a new representation scheme. Traditional attack graphs encode the entire network at each state, but the representation presented by the authors uses logical statements to represent a portion of the network at each node. This is called a logical attack graph. This approach led to the reduction of the generation process to quadratic time and reduced the number of nodes in the resulting graph to $\mathcal{O}(n^2)$. However, this approach does require more analysis for identifying attack vectors. Another approach presented by the authors of [13] represents a description of systems and their qualities and topologies as a state, with a queue of unexplored states. This work was continued by the authors of [14] by implementing a hash table among other features. Each of these works demonstrates an improvement in scalability through refining the desirable information output.

Another approach for generation improvement is through parallelization. The authors of [14] leverage OpenMP to parallelize the exploration of a FIFO queue. This parallelization also includes the utilization of OpenMP's dynamic scheduling. In this approach, each thread receives a state to explore, where a critical section is employed to handle the atomic functions of merging new state information while avoiding collisions, race conditions, or stale data usage. The authors measured a 10x speedup over the serial algorithm. The authors of [15] present a parallel generation approach using CUDA, where speedup is obtained through a large number of CUDA cores. For a distributed approach, the authors of [16] present a technique for utilizing reachability hyper-graph partitioning and a virtual shared memory abstraction to prevent duplicate work by multiple nodes. This work had promising results in terms of limiting the state-space explosion and speedup as the number of network hosts increases.

III. Necessary Components

A. Serialization

In order to distribute workloads across nodes in a distributed system, various types of data will need to be sent and received. Support and mechanisms vary based on the MPI implementation, but most fundamental data types such as integers, doubles, characters, and Booleans are incorporated into the MPI implementation. While this does simplify some of the messages that need to be sent and received in the MPI approaches of attack and compliance graph generation, it does not cover the vast majority of them when using RAGE.

RAGE implements many custom classes and structs that are used throughout the generation process. Qualities, topologies, network states, and exploits are a few such examples. Rather than breaking each of these down into fundamental types manually, serialization functions are leveraged to handle most of this. RAGE already incorporates Boost graph libraries for auxiliary support, so this work extended this further to utilize the serialization libraries also provided by Boost. These libraries also include support for serializing all STL classes, and many of the RAGE classes have members that make use of the STL classes. One additional advantage of the Boost library approach is that many of the RAGE classes are nested. For example, the NetworkState class has a member vector of Quality classes, and the Quality class has a Keyvalue class as a member. When serializing the NetworkState class, Boost will recursively serialize all members, including the custom class members, assuming they also have serialization functions.

When using the serialization libraries, this work opted to use the intrusive route, where the class instances are altered directly. This was preferable to the non-intrusive approach, since the class instances were able to be altered with relative ease, and many of the class instances did not expose enough information for the non-intrusive approach to be viable.

IV. Implementation of the Tasking Approach

The high-level overview of the attack and compliance graph generation process can be broken down into six main tasks. These tasks are described in Figure 1. Prior works such as that seen by the authors of [14], [15], and [16] work to parallelize the graph generation using OpenMP, CUDA, and hyper-graph partitioning. This approach, however, utilizes Message Passing Interface (MPI) to distribute the six identified tasks of RAGE to examine the effect on speedup, efficiency, and scalability for attack and compliance graph generation.

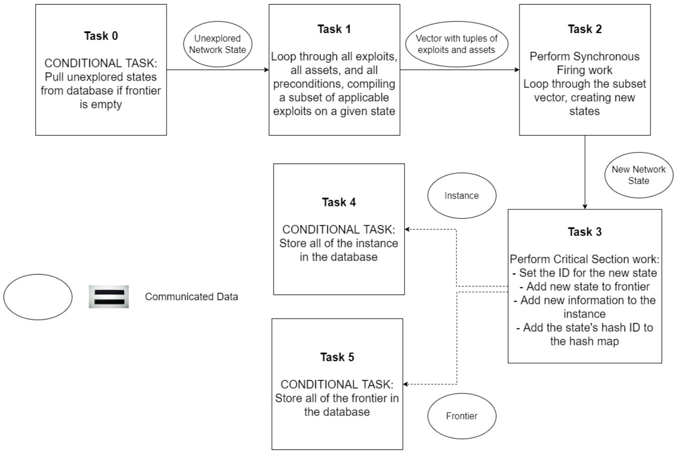
Task 0
CONDITIONAL TASK: Pull unexplored states from database if frontier is empty
Unexplored Network State
Task 1
Loop through all exploits, all assets, and all preconditions, compiling a subset of applicable exploits on a given state
Vector with tuples of exploits and assets
Task 2
Perform Synchronous Firing work
Loop through the subset vector, creating new states
New Network State
Task 3
Perform Critical Section work:
- Set the ID for the new state
- Add new state to frontier
- Add new information to the instance
- Add the state's hash ID to the hash map
Instance
Task 4
CONDITIONAL TASK: Store all of the instance in the database
Frontier
Task 5
CONDITIONAL TASK: Store all of the frontier in the database
Communicated Data

Fig. 1. Task Overview of the Attack and Compliance Graph Generation Process

A. Algorithm Design

The design of the tasking approach is to leverage a pipeline structure with the six tasks and MPI nodes. After its completion, each stage of the pipeline will pass the necessary data to the next stage through various MPI messages, where the next stage's nodes will receive the data and execute their tasks. The pipeline is considered fully saturated when each task has a dedicated node solely for executing work for that task. When there are less nodes than tasks, some nodes will process multiple tasks. When there are more nodes than tasks, additional nodes will be assigned to Tasks 1 and 2. Timings were collected in the serial approach for various networks that displayed more time requirements for Tasks 1 and 2, with larger network sizes requiring vastly more time to be taken in Tasks 1 and 2. As a result, additional nodes are assigned to Tasks 1 and 2. Node allocation can be seen in Figure 2. In this Figure, "world.size()" is an integer value representing the number of nodes used in the program, and "num_tasks" is an integer value representing the number of tasks used in the pipeline. By using a variable for the number of tasks, it allows for modular usage of the pipeline, where tasks can be added and removed without needing to change any allocation logic work; only communication between tasks may need to be modified, and the allocation can be adjusted relatively simply to include new tasks.

For determining which tasks should be handled by the root note, a few considerations were made, where minimizing communication cost and avoiding unnecessary complexity were the main two considerations. In the serial approach, the frontier queue was the primary data structure for the majority of the generation process. Rather than using a distributed queue or passing multiple sub-queues between nodes, the minimum cost option is to pass states individually. This approach also assists in reducing the complexity. Managing multiple frontier queues would require duplication checks, multiple nodes requesting data from and storing data into the database, and devising a strategy to maintain proper queue ordering, all of which would also increase the communication cost. As a result, the root node will be dedicated to Tasks 0 and 3.

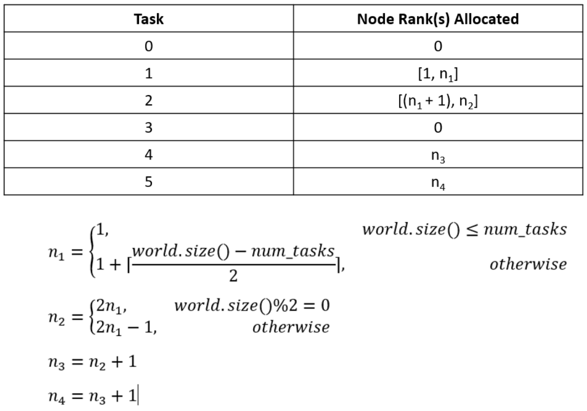

Task	Node Rank(s) Allocated
0	0
1	[1, n_1]
2	[(n_1 + 1), n_2]
3	0
4	n_3
5	n_4

$$n_1 = \begin{cases} 1, & world.size() \le num\_tasks \\ 1 + \lceil \frac{world.size() - num\_tasks}{2} \rceil, & otherwise \end{cases}$$

$$n_2 = \begin{cases} 2n_1, & world.size()\%2 = 0 \\ 2n_1 - 1, & otherwise \end{cases}$$

$$n_3 = n_2 + 1$$

$$n_4 = n_3 + 1$$

Fig. 2. Node Allocation for each Task

B. Communication Structure

The underlying communication structure for the tasking approach relies on a pseudo-ring structure. As seen in Figure 2, nodes n_2, n_3, and n_4 are derived from the previous task's greatest node rank. To keep the development abstract, a custom send function checks the world size ("world.size()") before sending. If the rank of the node that would receive a message is greater than the world size and therefore does not exist, the rank would then be "looped around" and corrected to fit within the world size constraints. After the rank correction, the MPI Send function was then invoked with the proper node rank.

C. Task Breakdown

1) Task 0: Task 0 is performed by the root node, and is a conditional task; it is not guaranteed to be executed at each pipeline iteration. Task 0 is only executed when the frontier is empty, but the database still holds unexplored states. This occurs when there are memory constraints, and database storage is performed during execution to offload the demand, as discussed in Section **??**. After the completion of Task 0, the frontier has a state popped, and the root node sends the state to n_1. If the frontier is empty, the root node sends the finalize signal to all nodes.

2) Task 1: Task 1 begins by distributing the workload between nodes based on the local task communicator rank. Rather than splitting the exploit list at the root node and sending sub-lists to each node allocated to Task 1, each node checks its local communicator rank and performs a modulo operation with the number of nodes allocated to determine whether it should proceed with the current iteration of the exploit loop. Since the exploit list is static, each node has the exploit list initialized prior to the generation process, and communication cost can be avoided from sending sub-lists to each node. Each node in Task 1 works to compile a reduced exploit list that is applicable to the current network state. A breakdown of the Task 1 distribution can be seen in Figure 3.

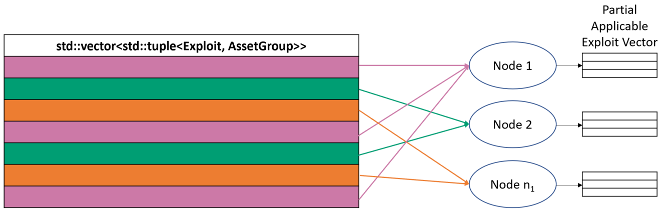

Fig. 3. Data Distribution of Task One

Once the computation work of Task 1 is completed, each node must send their compiled applicable exploit list to Task 2. Rather than merging all lists and splitting them back out in Task 2, each node in Task 1 will send an applicable exploit list to at most one node allocated to Task 2. Based on the allocation of nodes seen in Figure 2, there are 2 potential cases: the number of nodes allocated to Task 1 is equal to the number of nodes allocated to Task 2, or the number of nodes allocated to Task 1 is one greater than the number of nodes allocated to Task 2. For the first case, each node in Task 1 sends the applicable exploit list to its global rank+n_1. This case can be seen in Figure 4. For the second case, since there are more nodes allocated to Task 1 than Task 2, node n_1 scatters its partial applicable exploit list in the local Task 1 communicator, and all other Task 1 nodes follow the same pattern seen in the first case. This second case can be seen in Figure 5.

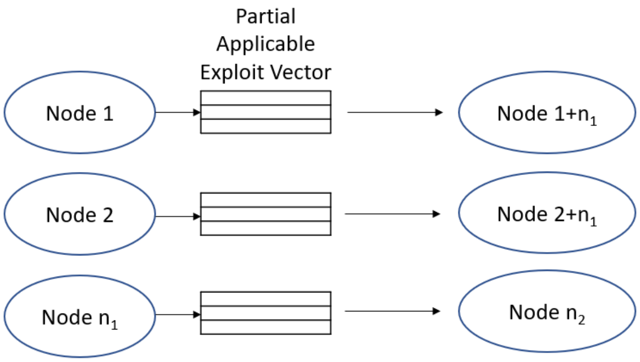

Fig. 4. Communication From Task 1 to Task 2 when the Number of Nodes Allocated is Equal

3) Task 2: Each node in Task 2 iterates through the received partial applicable exploit list and creates new states with edges

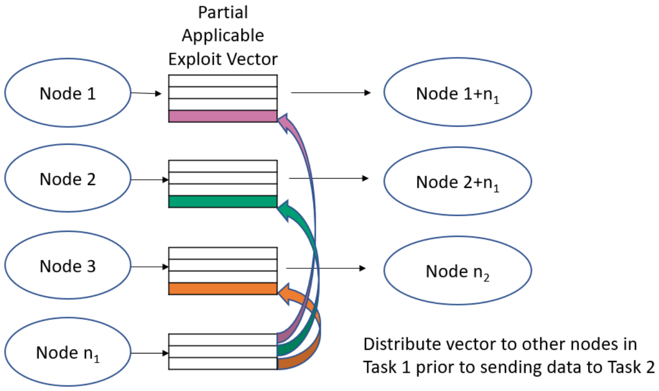
Partial Applicable Exploit Vector
Node 1
Node 2
Node 3
Node n_1
Node $1+n_1$
Node $2+n_1$
Node n_2
Distribute vector to other nodes in Task 1 prior to sending data to Task 2

Fig. 5. Communication From Task 1 to Task 2 when Task 1 Has More Nodes Allocated

Tag	Description
2	Task 2 Finalize Signal
3	Fact for Hash Map Update
4	NetworkState for Hash Map Update
5	NetworkState to be Added to the Frontier
6	Current NetworkState Reference for Edge Creation
7	Factbases for Task 4
8	Edges for Task 4
9	Group Exploit Vectors for Local Root in Task 2
10	Exploit Reference for Task 3 Work
11	AssetGroup Reference for Task 3 Work
14	Continue Signal
15	Finalize Signal
20	Current NetworkState Reference for Task 1
21	Applicable Exploit Vector Scatter for Task 1 Case 2
30	Applicable Exploit Vector Send to Task 2
40	NetworkState Send to Task 2
50	NetworkState to Store in Task 5

TABLE I
MPI TAGS FOR THE MPI TASKING APPROACH

to the current state. However, synchronous firing work is performed during this task, and syncing multiple exploits that could be distributed across multiple nodes leads to additional overhead and complexity. To prevent these difficulties, each node checks its partial applicable exploit list for exploits that are part of a group, removes these exploits from its list, and sends the exploits belonging to a group to the Task 2 local communicator root. Since the Task 2 local root now contains all group exploits, it can execute the Synchronous Firing work without additional communication or synchronization between other MPI nodes in the Task 2 stage. Other than the additional setup steps required for Synchronous Firing for the local root, all work performed during this task by all MPI nodes is that seen from the Synchronous Firing figure (Figure **??**).

4) Task 3: Task 3 is performed only by the root node, and no division of work is necessary. The root node will continuously check for new states until the Task 2 finalize signal is detected. This task consists of setting the new state's ID, adding it to the frontier, adding its information to the instance, and inserting information into the hash map. When the root node has processed all states and has received the Task 2 finalize signal, it will complete Task 3 by sending the instance and/or frontier to Task 4 and/or 5, respectively if applicable, then proceed to Task 0.

5) Task 4 and Task 5: Intermediate database operations, though not frequent and may never occur for small graphs, are lengthy and time-consuming when they do occur. As discussed in Section **??**, the two main memory consumers are the frontier and the instance, both of which are contained by the root node's memory. Since the database storage requests are blocking, the pipeline would halt for a lengthy period of time while waiting for the root node to finish potentially two large storages. Tasks 4 and 5 work to alleviate the stall by executing independently of the regular pipeline execution flow. Since Tasks 4 and 5 do not send any data, no other tasks must wait for these tasks to complete. The root node can then asynchronously send the frontier and instance to the appropriate nodes as needed, clear its memory, and continue execution without delay. After initial testing, it was determined that the communication cost of the asynchronous sending of data for Tasks 4 and 5 is less than the time requirement of a database storage operation if performed by the root node.

D. MPI Tags

To ensure that the intended message is received by each node, the MPI message envelopes have their tag fields specified. When a node sends a message, it specifies a tag that corresponds with the data and intent for which it is sent. The tag values were arbitrarily chosen, and tags can be added to the existing list or removed as desired. When receiving a message, a node can specify to only look for messages that have an envelope with a matching tag field. Not only do tags ensure that nodes are receiving the correct messages, they also reduce complexity for program design. Table I displays the list of tags used for the MPI Tasking approach.

V. PERFORMANCE EXPECTATIONS AND USE CASES

Due to the amount of communication between nodes to distribute the necessary data through all stages of the tasking pipeline, this approach is not expected to outperform the serial approach in all cases. This tasking approach was specifically designed to reduce the computation time when the generation of each individual state increases in time. This approach does not offer any guarantees of processing through the frontier at an increased rate; it's main objective is to distribute the workload of individual state generation. As discussed in Section **??**, the amount of entries in the National Vulnerability database and any custom vulnerability testing to ensure adequate examination of all assets in the network sums to large number of exploits in the exploit list. Likewise for compliance graphs and compliance examinations, Section **??** discussed that the number of compliance checks for SOX, HIPAA, GDPR, PCI DSS, and/or any other regulatory compliance also sums to a large number of compliance checks in the exploit list. Since the generation of each state is largely

Task	Shortened Description	Performance Affected By
0	Retrieve Next State	Database Load
1	Compile List of Applicable Exploits	Number of Exploits
2	Loop through List of Applicable Exploits	Number of Applicable Exploits
3	Bookkeeping	Number of States
4	C/R and/or memory clear of graph instance	Database Load
5	C/R and/or memory clear of frontier	Database Load

TABLE II
TASK DESCRIPTIONS AND PERFORMANCE NOTES

dependent on the number of exploits present in the exploit list, this approach is best-suited for when the exploit list grows in size. As will be later discussed, it is also hypothesized that this approach is well-suited when many database operations occur.

VI. EXPERIMENTAL SETUP

In order to capture a comprehensive image of the tasking approach's impact on performance, a number of parameters were altered and the generation properties were examined. Table II presents each task and the parameters that affect the performance of each task. Generating larger graphs would increase the runtime, but does not necessarily stress each task or provide a consistent, reliable way to draw conclusions regarding the tasking approach. In order to ensure consistency across the experimental testing and minimize the possibility of introducing bias, all tests generated the exact same graph. All tests would generate the same graph with identical numbers of states, identical numbers of edges, identical labeling, and identical inner workings and underlying properties. The following subsections describe the altered parameters, the manner in which they were altered, and how data integrity of the resulting graph was preserved. The parameter alteration process focused on avoiding artificial inflation of the performance metrics, and each subsection emphasizes the practicality of each altered parameter.

A. *Number of Exploits*

B. *Applicability of Exploits*

C. *Database Load*

D. *Testing Platform*

All data was collected on a 13 node cluster, with 12 nodes serving as dedicated compute nodes, and 1 node serving as the login node. Each compute node has a configuration as follows:

- OS: CentOS release 6.9
- CPU: Two Intel Xeon E5-2620 v3
- Two Intel Xeon Phi Co-Processors
- One FPGA (Nallatech PCIE-385n A7 Altera Stratix V)
- Memory: 64318MiB

All nodes are connected with a 10Gbps Infiniband interconnect.

VII. RESULTS

A series of tests were conducted on the platform described at the beginning of Section **??**, and results were collected in regards to the effect of the MPI Tasking approach on increasing sizes of exploit lists for a varying number of nodes. The exploit list initially began with 6 items, and each test scaled the number of exploits by a factor of 2. The final test was with an exploit list with 49,512 entries. If all of the items in these exploit lists were applicable, the runtime would be too great for feasible testing due to the state space explosion. To prevent state-space explosion but still gather valid results, each exploit list in the tests contained 6 exploits that could be applicable, and all remaining exploits were not applicable. The not applicable exploits were created in a fashion similar to that seen in Figure 6. By creating a multitude of not applicable exploits, testing can safely be conducted by ensuring state space explosion would not occur while still observing the effectiveness of the tasking approach.

The results of the Tasking Approach can be seen in Figure 7. In terms of speedup, when the number of entries in the exploit list is small, the serial approach has better performance. This is expected due to the communication cost requiring more time than it does to generate a state, as discussed in Section V. However, as the number of items in the exploit list increase, the Tasking Approach quickly begins to outperform the serial approach. It is notable that even when the tasking pipeline is not fully saturated (when there are less compute nodes assigned than tasks), the performance is still approximately equal to that of the serial approach. The other noticeable feature is that as more compute nodes are assigned, the speedup continues to increase.

In terms of efficiency, 2 compute nodes offer the greatest value since the speedup using 2 compute nodes is approximately 1.0 as the exploit list size increases. While the 2 compute node option does offer the greatest efficiency, it does not provide a speedup greater than 1.0 on any of the testing cases conducted. The results also demonstrate that an odd number of compute nodes in a fully saturated pipeline has better efficiency that an even number of compute nodes. When referring to Figure 2, when there is an odd number number of compute nodes, Task 1 is allocated more nodes than Task 2. In the testing conducted, Task 1 was responsible for iterating through an increased size of the exploit list, so more nodes is advantageous in distributing the workload. However, since many exploits were not applicable, Task 2 had a lower workload where only 6 exploits could be applicable. This will be further elaborated upon in Section **??**, but it is expected that efficiency will increase for real networks, since nodes in Task 2 will see a realistic workload.

Figures 8, 9, and 10 display the results of the tasking approach for runtime in milliseconds, speedup, and efficiency respectively in table format.

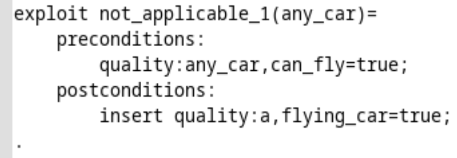

```
exploit not_applicable_1(any_car)=
    preconditions:
        quality:any_car,can_fly=true;
    postconditions:
        insert quality:a,flying_car=true;
.
```

Fig. 6. Example of a Not Applicable Exploit for the MPI Tasking Testing

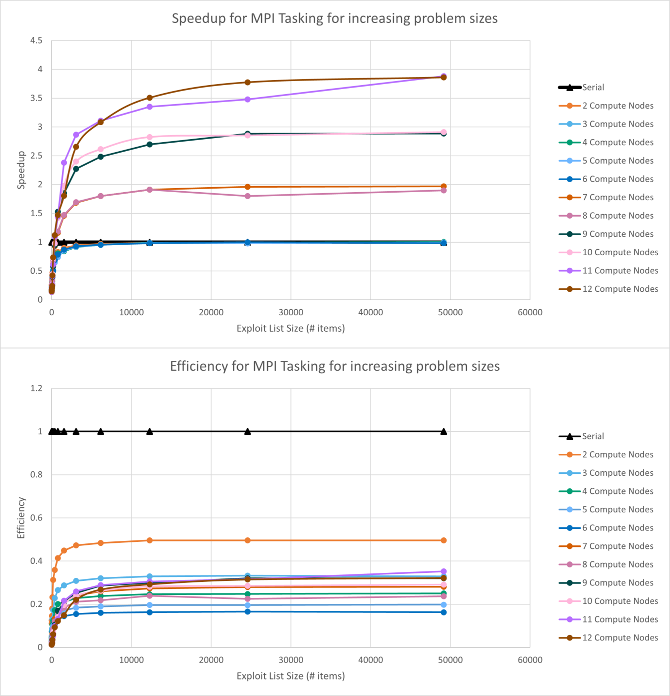

Fig. 7. Speedup and Efficiency of the MPI Tasking Approach for a Varying Number of Compute Nodes with an Increasing Problem Size

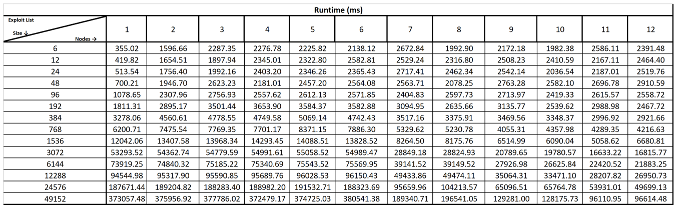

	Runtime (ms)											
Exploit List Size ↓ Nodes →	1	2	3	4	5	6	7	8	9	10	11	12
6	355.02	1596.66	2287.35	2276.78	2225.82	2138.12	2672.84	1992.90	2172.18	1982.38	2586.11	2391.48
12	419.82	1654.51	1897.94	2345.01	2322.80	2582.81	2529.24	2316.80	2508.23	2410.59	2167.11	2464.40
24	513.54	1756.40	1992.16	2403.20	2346.26	2365.43	2717.41	2462.34	2542.14	2036.54	2187.01	2519.76
48	700.21	1946.70	2623.23	2181.01	2457.20	2564.08	2563.71	2078.25	2763.28	2582.10	2696.78	2910.59
96	1078.65	2307.96	2756.93	2557.62	2612.13	2571.85	2404.83	2597.73	2713.97	2419.33	2615.57	2558.72
192	1811.31	2895.17	3501.44	3653.90	3584.37	3582.88	3094.95	2635.66	3135.77	2539.62	2988.98	2467.72
384	3278.06	4560.61	4778.55	4749.58	5069.14	4742.43	3517.16	3375.91	3469.56	3348.37	2996.92	2921.66
768	6200.71	7475.54	7769.35	7701.17	8371.15	7886.30	5329.62	5230.78	4055.31	4357.98	4289.35	4216.63
1536	12042.06	13407.58	13968.34	14293.45	14088.51	13828.52	8264.50	8175.76	6514.99	6090.04	5058.62	6680.81
3072	53293.52	54362.74	54779.59	54991.61	55058.52	54989.47	28849.18	28824.93	20789.65	19780.57	16633.22	16815.77
6144	73919.25	74840.32	75185.22	75340.69	75543.52	75569.95	39141.52	39149.52	27926.98	26625.84	22420.52	21883.25
12288	94544.98	95317.90	95590.85	95689.76	96028.53	96150.43	49433.86	49474.11	35064.31	33471.10	28207.82	26950.73
24576	187671.44	189204.82	188283.40	188982.20	191532.71	188323.69	95659.96	104213.57	65096.51	65764.78	53931.01	49699.13
49152	373057.48	375956.92	377786.02	372479.17	374725.03	380541.38	189340.71	196541.05	129281.00	128175.73	96110.95	96614.48

Fig. 8. Results for the MPI Tasking Approach in Terms of Runtime in Milliseconds

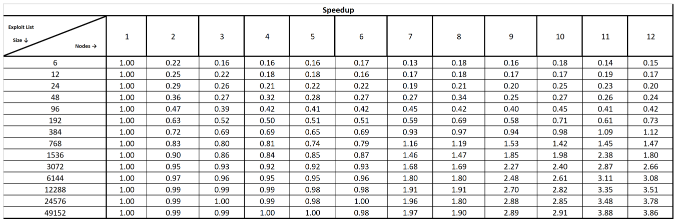

	Speedup											
Exploit List Size ↓ Nodes →	1	2	3	4	5	6	7	8	9	10	11	12
6	1.00	0.22	0.16	0.16	0.16	0.17	0.13	0.18	0.16	0.18	0.14	0.15
12	1.00	0.25	0.22	0.18	0.18	0.16	0.17	0.18	0.17	0.17	0.19	0.17
24	1.00	0.29	0.26	0.21	0.22	0.22	0.19	0.21	0.20	0.25	0.23	0.20
48	1.00	0.36	0.27	0.32	0.28	0.27	0.27	0.34	0.25	0.27	0.26	0.24
96	1.00	0.47	0.39	0.42	0.41	0.42	0.45	0.42	0.40	0.45	0.41	0.42
192	1.00	0.63	0.52	0.50	0.51	0.51	0.59	0.69	0.58	0.71	0.61	0.73
384	1.00	0.72	0.69	0.69	0.65	0.69	0.93	0.97	0.94	0.98	1.09	1.12
768	1.00	0.83	0.80	0.81	0.74	0.79	1.16	1.19	1.53	1.42	1.45	1.47
1536	1.00	0.90	0.86	0.84	0.85	0.87	1.46	1.47	1.85	1.98	2.38	1.80
3072	1.00	0.95	0.93	0.92	0.92	0.93	1.68	1.69	2.27	2.40	2.87	2.66
6144	1.00	0.97	0.96	0.95	0.95	0.96	1.80	1.80	2.48	2.61	3.11	3.08
12288	1.00	0.99	0.99	0.99	0.98	0.98	1.91	1.91	2.70	2.82	3.35	3.51
24576	1.00	0.99	1.00	0.99	0.98	1.00	1.96	1.80	2.88	2.85	3.48	3.78
49152	1.00	0.99	0.99	1.00	1.00	0.98	1.97	1.90	2.89	2.91	3.88	3.86

Fig. 9. Results for the MPI Tasking Approach in Terms of Speedup

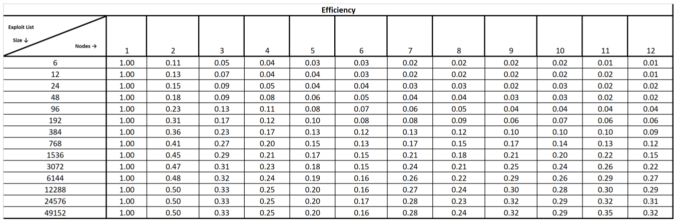

	Efficiency											
Exploit List Size ↓ Nodes →	1	2	3	4	5	6	7	8	9	10	11	12
6	1.00	0.11	0.05	0.04	0.03	0.03	0.02	0.02	0.02	0.02	0.01	0.01
12	1.00	0.13	0.07	0.04	0.04	0.03	0.02	0.02	0.02	0.02	0.02	0.01
24	1.00	0.15	0.09	0.05	0.04	0.04	0.03	0.03	0.02	0.03	0.02	0.02
48	1.00	0.18	0.09	0.08	0.06	0.05	0.04	0.04	0.03	0.03	0.02	0.02
96	1.00	0.23	0.13	0.11	0.08	0.07	0.06	0.05	0.04	0.04	0.04	0.04
192	1.00	0.31	0.17	0.12	0.10	0.08	0.08	0.09	0.06	0.07	0.06	0.06
384	1.00	0.36	0.23	0.17	0.13	0.12	0.13	0.12	0.10	0.10	0.10	0.09
768	1.00	0.41	0.27	0.20	0.15	0.13	0.17	0.15	0.17	0.14	0.13	0.12
1536	1.00	0.45	0.29	0.21	0.17	0.15	0.21	0.18	0.21	0.20	0.22	0.15
3072	1.00	0.47	0.31	0.23	0.18	0.15	0.24	0.21	0.25	0.24	0.26	0.22
6144	1.00	0.48	0.32	0.24	0.19	0.16	0.26	0.22	0.29	0.26	0.29	0.27
12288	1.00	0.50	0.33	0.25	0.20	0.16	0.27	0.24	0.30	0.28	0.30	0.29
24576	1.00	0.50	0.33	0.25	0.20	0.17	0.28	0.23	0.32	0.29	0.32	0.31
49152	1.00	0.50	0.33	0.25	0.20	0.16	0.28	0.24	0.32	0.29	0.35	0.32

Fig. 10. Results for the MPI Tasking Approach in Terms of Efficiency

VIII. Analysis

IX. Conclusion

References

[1] P. Pacheco, *An Introduction to Parallel Programming*. Morgan Kaufmann, print ed., 2011.

[2] S. Ainsworth and T. M. Jones, "Graph prefetching using data structure knowledge," *Proceedings of the International Conference on Supercomputing*, vol. 01-03-June, 2016.

[3] P. Yao, L. Zheng, X. Liao, H. Jin, and B. He, "An efficient graph accelerator with parallel data conflict management," *Parallel Architectures and Compilation Techniques - Conference Proceedings, PACT*, 2018.

[4] J. Zhang, S. Khoram, and J. Li, "Boosting the performance of FPGA-based graph processor using hybrid memory cube: A case for breadth first search," *FPGA 2017 - Proceedings of the 2017 ACM/SIGDA International Symposium on Field-Programmable Gate Arrays*, pp. 207–216, 2017.

[5] G. Dai, Y. Chi, Y. Wang, and H. Yang, "FPGP: Graph processing framework on FPGA: A case study of breadth-first search," *FPGA 2016 - Proceedings of the 2016 ACM/SIGDA International Symposium on Field-Programmable Gate Arrays*, pp. 105–110, 2016.

[6] S. Arifuzzaman and M. Khan, "Fast parallel conversion of edge list to adjacency list for large-scale graphs," in *HPC '15: Proceedings of the Symposium on High Performance Computing*, pp. 17–24, Apr. 2015.

[7] X. Yu, W. Chen, J. Miao, J. Chen, H. Mao, Q. Luo, and L. Gu, "The Construction of Large Graph Data Structures in a Scalable Distributed Message System," in *HPCCT 2018: Proceedings of the 2018 2nd High Performance Computing and Cluster Technologies Conference*, pp. 6–10, June 2018.

[8] P. Liakos, K. Papakonstantinopoulou, and A. Delis, "Memory-Optimized Distributed Graph Processing through Novel Compression Techniques," in *CIKM '16: Proceedings of the 25th ACM International Conference on Information and Knowledge Management*, pp. 2317–2322, Oct. 2016.

[9] J. Balaji and R. Sunderraman, "Graph Topology Abstraction for Distributed Path Queries," in *HPGP '16: Proceedings of the ACM Workshop on High Performance Graph Processing*, pp. 27–34, May 2016.

[10] "An Overview of the Parallel Boost Graph Library - 1.75.0," 2009.

[11] J. Siek, L.-Q. Lee, and A. Lumsdaine, "The Boost Graph Library, vers. 1.75.0." https://www.boost.org/doc/libs/1_75_0/libs/graph/doc/index.html.

[12] X. Ou, W. F. Boyer, and M. A. Mcqueen, "A Scalable Approach to Attack Graph Generation," *CCS '06: Proceedings of the 13th ACM conference on Computer and communications security*, pp. 336–345, 2006.

[13] K. Cook, T. Shaw, J. Hale, and P. Hawrylak, "Scalable attack graph generation," *Proceedings of the 11th Annual Cyber and Information Security Research Conference, CISRC 2016*, 2016.

[14] M. Li, P. Hawrylak, and J. Hale, "Concurrency Strategies for Attack Graph Generation," *Proceedings - 2019 2nd International Conference on Data Intelligence and Security, ICDIS 2019*, pp. 174–179, 2019.

[15] M. Li, P. J. Hawrylak, and J. Hale, "Implementing an attack graph generator in cuda," in *2020 IEEE International Parallel and Distributed Processing Symposium Workshops (IPDPSW)*, pp. 730–738, 2020.

[16] K. Kaynar and F. Sivrikaya, "Distributed attack graph generation," *IEEE Transactions on Dependable and Secure Computing*, vol. 13, no. 5, pp. 519–532, 2016.